Eur Biophys J (2008) 37:1145–1156
DOI 10.1007/s00249-008-0267-2

ORIGINAL PAPER

Effects of changes in extracellular pH and potassium concentration on Kv1.3 inactivation

Sándor Somodi · Péter Hajdu · Rezső Gáspár · György Panyi · Zoltán Varga

Received: 1 October 2007 / Revised: 22 December 2007 / Accepted: 8 January 2008 / Published online: 24 January 2008

Abstract The Kv1.3 channel inactivates via the P/C-type mechanism, which is influenced by a histidine residue in the pore region (H399, equivalent of Shaker 449). Previously we showed that the electric field of the protonated histidines at low extracellular pH (pH_e) creates a potential barrier for K^+ ions just outside the pore that hinders their exit from the binding site controlling inactivation (control site) thereby slowing inactivation kinetics. Here we examined the effects of extracellular potassium $[K^+]_e$ and pH_e on the rate of inactivation of Kv1.3 using whole-cell patch-clamp. We found that in 150 mM $[K^+]_e$ inactivation was accelerated upon switching to pH_e 5.5 as opposed to the slowing at 5 mM $[K^+]_e$. The transition from slowing to acceleration occurred at 40 mM $[K^+]_e$, whereas this "turning point" was at 20 mM $[K^+]_e$ for inward currents. The rate of entry of Ba^{2+} ions from the extracellular space to the control site was significantly slowed by low pH_e in wild-type hKv1.3, but it was insensitive to pH_e in H399K and H399L mutants. Based on these observations we expanded our model and propose that the potential barrier created by the protonated histidines impedes the passage of K^+ ions between the extracellular medium and the control site in both directions and the effect on inactivation rate (acceleration or slowing) depends on the relative contribution of filling from the extracellular and intracellular sides.

Regional Biophysics Conference of the National Biophysical Societies of Austria, Croatia, Hungary, Italy, Serbia, and Slovenia.

S. Somodi · P. Hajdu · R. Gáspár · G. Panyi (✉) · Z. Varga
Department of Biophysics and Cell Biology,
Research Center for Molecular Medicine,
Medical and Health Science Center, University of Debrecen,
Nagyerdei krt. 98, 4012 Debrecen, Hungary
e-mail: panyi@jaguar.dote.hu

Keywords Potassium channel · Inactivation · Extracellular pH · Extracellular K^+ concentration · Barium block · K^+ binding site

Introduction

Inactivation is an inherent property of many voltage-gated K^+ channels that controls the K^+ permeability of the cell membrane in both excitable and non-excitable cells. Shaker-related potassium channels have two distinct inactivation mechanisms, the N-type and the P/C-type. N-type inactivation is mediated by a tethered inactivation particle at the N-terminus of each channel subunit (Hoshi et al. 1990; Zagotta et al. 1990; Hoshi et al. 1991), while P/C-type inactivation occurs near the extracellular mouth of the channel by first preventing K^+ permeation, then eventually influencing the voltage-sensing machinery (Choi et al. 1991; Liu et al. 1996; Nguyen et al. 1996; Olcese et al. 1997; Loots and Isacoff 1998; Loots and Isacoff 1998). Although it is not the C-terminus of the channel where the structural changes take place, the process has been traditionally called C-type inactivation, and as new results from voltage-clamp fluorometry implicated the involvement of the selectivity filter in the phenomenon it has been renamed "P/C-type", the "P" coming from the "pore region" (Loots and Isacoff 1998; Loots and Isacoff 2000). This process is genrally slower than the N-type; consequently it is also referred to as slow inactivation. The rate of the P/C-type inactivation is sensitive to the ionic composition and pH of the extracellular solution (López-Barneo et al. 1993) and it can also be modulated by channel blockers, for example, tetraethylammonium (TEA)(Choi et al. 1991). Both high extracellular $[K^+]$ and extracellular TEA were suggested to slow the rate of inactivation via the

"foot in the door" mechanism (López-Barneo et al. 1993; Baukrowitz and Yellen 1995, 1996). This means that the rate of inactivation depends on the occupancy of a critical potassium binding site in the pore. The higher occupancy of this binding site delays the conformational rearrangements leading to inactivation. More recently this view was challenged for TEA by experiments that showed that TEA does not enter the pore as deeply as proposed earlier (Heginbotham and MacKinnon 1992) and thus does not itself act as the foot in the door, but may prevent the exit of a K^+ ion from the control site positioned more deeply (Andalib et al. 2004). This binding site is believed to be the outermost of the four K^+ binding sites in the selectivity filter (site #1 using the numbering of Zhou et al. 2001) whose filling at high extracellular [K^+] from the extracellular space is increased, consequently leading to higher occupancy and slower inactivation kinetics (Yellen 1998; Kiss and Korn 1998; Harris et al. 1998; Neyton and Miller 1988; Kiss et al. 1999; Ogielska and Aldrich 1999; Zhou et al. 2001). The occupancy of this binding site depends not only on the extracellular [K^+], but also on the filling of the binding site from the intracellular side. This fact was confirmed by two experiments: First, N-type inactivation accelerates P/C-type inactivation, because the occlusion of the internal mouth of the channel inhibits outward K^+ flux, which normally fills the control site. The reduced filling from the intracellular side results in the acceleration of P/C-type inactivation (Baukrowitz and Yellen 1995). Second, use-dependent intracellular blockers of the Shaker channel increase the rate of P/C-type inactivation. The acceleration of inactivation depends on the lifetime of the drug-bound form of the channel (Baukrowitz and Yellen 1996).

Mutations in the pore region can also influence the rate of slow inactivation. In Shaker the amino acid at position 449 is critical because its replacement significantly alters the rate of slow inactivation (López-Barneo et al. 1993). In Shaker-related channels (Kv1.3, Kv1.4) the replacement of the equivalent amino acid also caused a drastic change of the inactivation rate (Nguyen et al. 1996; Claydon et al. 2000; Li et al. 2003; Somodi et al. 2004), although in some cases such mutations had much weaker effects (Rasmusson et al. 1995; Fedida et al. 1999). So in most cases the identity of the Shaker 449 equivalent residue is an important, but definitely not the sole determinant of the inactivation rate.

Several studies have investigated the pH-dependence of inactivation in various wildtype and mutant K^+ channels. Lowering pH_e accelerated the rate of inactivation in wild-type Shaker and several of its mutants, wild-type Kv1.5 and Kv1.4 and in five Kv1.3 mutants. In these studies two critical locations have been pinpointed as responsible for conveying pH sensitivity to inactivation: the equivalent residues of Shaker 449 at the extracellular mouth of the pore and those corresponding to Shaker 425 in the turret region. Mutations at these positions in any of the host channels affected the pH-dependence of inactivation and evidence for the interaction between this pair of residues was also found (López-Barneo et al. 1993; Perez-Cornejo 1999; Steidl and Yool 1999; Kehl et al. 2002; Claydon et al. 2002, 2004; Starkus et al. 2003; Li et al. 2003; Somodi et al. 2004; Zhang et al. 2005). In addition to accelerating inactivation external acidification was also reported to reduce the current amplitude in most cases as well. This effect was attributed in part to the enhanced rate of inactivation from the open state and in part to closed-state inactivation (Starkus et al. 2003; Zhang et al. 2005; Claydon et al. 2007).

However, in none of these studies was slowing of inactivation at low pH_e observed as it was described for wild-type Kv1.3 bearing a histidine (H399) at the Shaker equivalent 449. This unique feature of human Kv1.3 was first reported almost two decades ago and was soon confirmed on rat channels as well (Deutsch and Lee 1989; Busch et al. 1991), but until recently no model was suggested for this anomalous behavior.

In our previous study we examined the role of the critically positioned H399 in the pH regulation of inactivation (Somodi et al. 2004). Based on our results using mutant channels, high-ionic-strength solutions and the measurement of the dissociation rate of blocking Ba^{2+} ions we created a model to explain how H399 influences the pH-dependence of inactivation. The main hypothesis of the model is that the electric field of protonated histidine residues at position 399 creates a potential barrier at the external mouth of the channel that impedes the exit of potassium ions from the critical binding site controlling inactivation to the extracellular space in low pH_o (Somodi et al. 2004). This manifests as slower inactivation.

Increased $[K^+]_e$ is known to influence the rate of inactivation in K^+ channels and an interplay between $[K^+]_e$ and pH_e has also been reported (Kehl et al. 2002; Li et al. 2003; Claydon et al. 2004). In light of this, in the present study we examined the effect of extracellular acidification at different extra- and intracellular potassium concentrations on the inactivation of the hKv1.3 channel. Here we test the hypothesis that the potential barrier created by the electric field of the histidines at low pH_e also exists for ions entering the pore from the extracellular side. Thus, in conditions where the control site is likely to be filled from the outside this barrier is expected to reduce its occupancy and enhance inactivation. Besides using different K^+ concentrations we also examined the rate of entry of barium ions into the pore from the extracellular solution at different pH_e values to gather supporting evidence for our model.

Materials and methods

Cells

Cytotoxic murine T cells (CTLL-2) were transiently co-transfected with plasmids encoding the wild type Kv1.3 channel (pRc/CMV/WT) along with a Ccd4neo plasmid (gifts from Dr. Carol Deutsch, University of Pennsylvania. Philadelphia, PA), containing the gene for human membrane-surface CD4, at a molar ratio of 5:1 or 8:1 [32 or 48 μg/ml total DNA] using electroporation (Deutsch and Chen 1993). CTLL-2 cells were cultured in RPMI-1640 supplemented with 10% FBS (Hyclone, Logan, Utah), 2 mM Na pyruvate, 10 mM HEPES, 4 mM L-glutamine, 50 μM 2-mercaptoethanol, and 100 CU/ml IL-2. Before transfection, cells were cultured for 24 h in fresh medium and collected in the logarithmic phase of growth. After harvesting, cells were suspended in Hanks'-20 mM HEPES balanced salt solution (pH 7.23) at $2x10^7$ cells/ml, and the appropriate mixture of DNA was added to the cell suspension. This suspension was transferred to electroporation cuvettes (400 μl/cuvette, 4 mm electrode gap), kept on ice for 10 min, and then electroporated using a BTX-electroporator (San Diego, CA) with settings previously determined to give ~50% viability at 24 h post transfection (725 V/cm, 2350 μF, 13 Ω). The resultant time constants were 22–25 ms. Cells were incubated for an additional 10 min on ice, and transferred back to culture medium (~0.5×10^6 cells/ml) supplemented with 5 mM Na-butyrate (at 37°C, 5% CO_2). Cells were used for electrophysiology between 8–16 h after the transfection.

Electrophysiology

Whole-cell measurements were carried out using Axopatch-200 and Axopatch-200A amplifiers connected to personal computers using Axon Instruments TL-1-125 and Digidata 1200 computer interfaces, respectively. For data acquisition and analysis the pClamp6 and the pClamp8 software package (Axon Instruments Inc., Foster City, CA) were used. CD4 positive CTLL-2 cells were selected for current recording by incubation with mouse anti-human CD4 antibodies (0.5 μg/10^6 cells, AMAC, Westbrook), followed by selective adhesion to petri dishes coated with goat anti-mouse IgG antibody (Biosource, Camarilo, CA), as previously described by Matteson and Deutsch (Matteson and Deutsch 1984) and Deutsch and Chen (Deutsch and Chen 1993). Dishes were washed gently five times with 1 ml of normal extracellular bath medium (see below) before the patch-clamp experiments. Standard whole-cell patch-clamp techniques were used, as described previously (Hamill et al. 1981). Pipettes were pulled from GC150F-15 borosilicate glass capillaries (Clark Biomedical Instruments, UK) in five stages and fire-polished to give electrodes of 2–3 MΩ resistance in the bath. The standard extracellular solution (S-ECS) was (in mM): 145 NaCl, 5 KCl, 1 $MgCl_2$, 2.5 $CaCl_2$, 5.5 glucose, 10 HEPES (pH 7.35 using NaOH, 305 mOsm/kg). The pipette solution was (in mM): 140 KF, 11 EGTA, 1 $CaCl_2$, 2 $MgCl_2$, and 10 HEPES (pH 7.20 using KOH, ~295 mOsm/kg). Cells with low series resistance (2–5 MΩ) were used and series resistance compensation up to 85% was applied to minimize voltage errors and achieve good voltage clamp conditions. The uncompensated series resistance error was in the order of 5–10 mV. The reference electrode was connected to the recording chamber with an agar bridge to eliminate junction potential changes during perfusion.

Test substances

In external solutions with 20, 40 or 150 mM $[K^+]_e$ (20, 40 or 150 mM K-ECS), NaCl was partially or completely substituted by KCl to get the given $[K^+]_e$. In the 15-mM-Ba^{2+} solution NaCl was replaced by equimolar $BaCl_2$. Bath solutions having low pH (6.5, 5.5) were buffered with 10 mM MES instead of HEPES. When the effect of low $[K^+]_i$ was tested the pipette solution contained (in mM) the following: 140 NaF, 5 KF, 11 EGTA, 1 $CaCl_2$, 2 $MgCl_2$, and 10 HEPES (pH 7.20 using NaOH, ~295 mOsm/kg).

Bath perfusion with different test solutions was achieved using a gravity-flow perfusion setup with eight input lines and a PE10 polyethylene tube output tip with flanged aperture to reduce the turbulence of the flow. The solutions were applied in an alternating sequence of control and test solutions, unless stated otherwise. Excess fluid was removed continuously from the bath.

Data analysis

Prior to analysis whole cell current traces were corrected for ohmic leak and digitally filtered (three point boxcar smoothing). Non-linear least squares fits were done using the Marquardt-Levenberg algorithm. Fits were evaluated visually as well as by the residuals and the sum of squared differences between the measured and calculated data points. For the determination of the time constant of exponentially decaying current traces the first cursor was placed to 90% of the peak (on the declining phase), and the second cursor was placed to the end of the record where the current reached a steady-state value.

Because of the inherent acceleration of the rate of inactivation with time after achieving whole cell configuration, current decays were characterized (either using time constants or APPR, see the definition below) for control conditions both before and after treatment and the mean of these values was compared with the value obtained during

treatment. Paired comparisons were performed for each individual cell to exclude the effect of cell-to-cell variability of the inactivation rate.

Statistical comparisons were made using Analysis of Variance (ANOVA), student's *t* test, and when appropriate, paired *t* test at $P = 0.05$. For all experiments, the standard error of the mean (SE) is reported.

Results

Low external pH accelerates inactivation kinetics in high-extracellular-potassium solutions

In our earlier study we confirmed the original observation of Deutsch and Lee that the rate of slow (P/C-type) inactivation of Kv1.3 is slowed when extracellular pH (pH_e) is lowered in an extracellular solution containing 5 mM K^+ (Fig. 1a) (Deutsch and Lee 1989; Somodi et al. 2004). In this study we examined the effect of changes in pH_e on inactivation kinetics in extracellular solutions with high K^+ concentration.

Elevation of the external K^+ concentration is known to slow the rate of inactivation in various K^+ channels (López-Barneo et al. 1993; Baukrowitz and Yellen 1995; Baukrowitz and Yellen 1996). This is presumably due to the higher occupancy of the control site (López-Barneo et al. 1993; Baukrowitz and Yellen 1996; Harris et al. 1998). Moreover, the kinetics of inactivation of Kv1.3 channels becomes biphasic, so current decay can be characterized by a fast (τ_f) and a slow (τ_s) time constant (Grissmer and Cahalan 1989). This was seen in our records when the cell was perfused with K-ECS (high-K^+-concentration extracellular solution) pH 7.35, which contained 150 mM K^+: the fit containing two exponential terms yielded $\tau_f = 60.5 \pm 3.8$ ms ($n = 11$) and $\tau_s = 610 \pm 46$ ms ($n = 11$) for the fast and slow components, respectively. The relative weight of the amplitude of the slow inactivating current component was

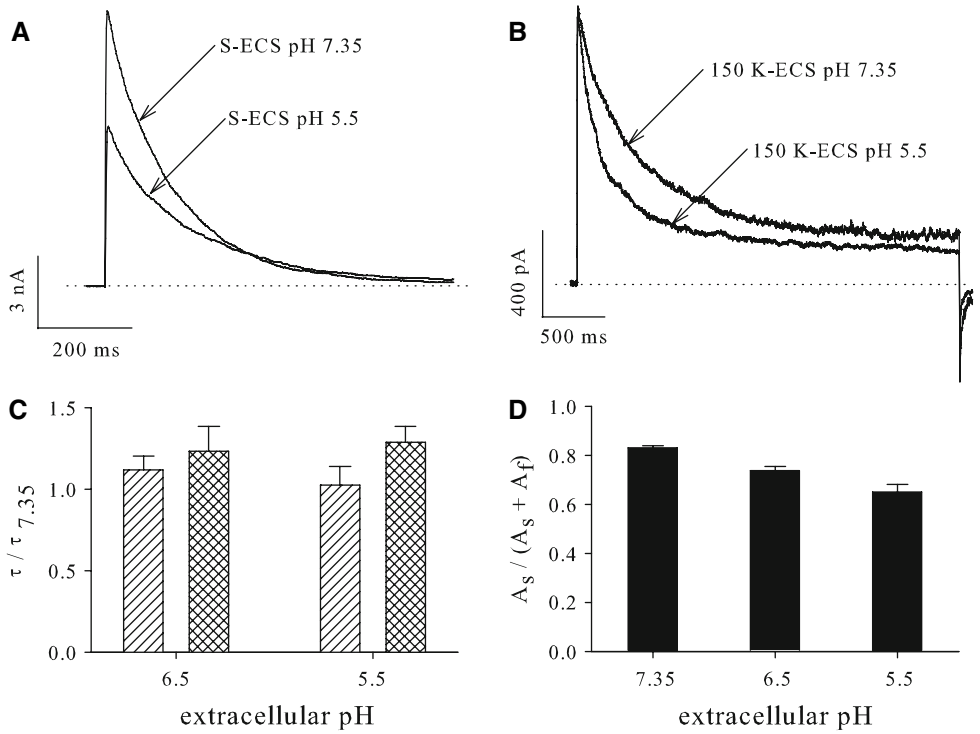

Fig. 1 Effect of extracellular pH on the inactivation kinetics of Kv1.3 currents at different $[K^+]_e$. **a** K^+ currents of a CTLL-2 cell expressing Kv1.3 channels were recorded in whole-cell configuration during 2 s-long test pulses to +50 mV from a holding potential of −120 mV. Test pulses were applied every 60 s. The bath was perfused with S-ECS ($[K^+]_e = 5$ mM), pH 7.35 or with S-ECS pH 5.5. For the cell shown, inactivation time constants were 142 and 184 ms at pH 7.35 and 5.5, respectively. Only the first 1,000 ms of the traces are shown. **b** K^+ currents of a CTLL-2 cell were recorded in whole-cell configuration during 3 s-long test pulses to +50 mV. The holding potential was −120 mV. Test pulses were applied every 90 s. The bath was perfused with K-ECS ($[K^+]_e = 150$ mM), pH 7.35 or with K-ECS, pH 5.5. The decay of the currents in K-ECS solutions could be fitted with the sum of two exponential terms: $I(t) = A_f \times \exp(-t/\tau_f) + A_s \times \exp(-t/\tau_s) + C$. The resulting time constants were $\tau_s = 506$ ms, $\tau_f = 76$ ms at pH 7.35; $\tau_s = 437$ ms, $\tau_f = 94$ ms at pH 5.5. **c** Inactivation time constants (τ_1 and τ_2) of whole-cell currents were determined in K-ECS ($\tau_{7.35}$) and in solutions having lower extracellular pH (τ) from double exponential fits to the decaying parts of current traces. The ratio of $\tau/\tau_{7.35}$ was calculated for $n = 7$ experiments at pH 6.5 and for $n = 10$ experiments at pH 5.5 for the slow (*hatched bar*) and fast (*cross-hatched bar*) component. Error bars indicate SE. **d** The relative weight of the slow component of the decay was expressed as $A_s/(A_s + A_f)$ where A_s and A_f are the amplitudes of the slow and fast components of decay, respectively, at pH 7.35, 6.5 and 5.5

higher than the weight of the fast inactivating component, the ratio of $A_s/(A_s + A_f)$ was 0.830 ± 0.011 ($n = 11$).

We examined the effect of pH_e on the rate of inactivation in K-ECS. In contrast to the slowing seen in low external K^+ the inactivation of Kv1.3 current became faster in low pH_e (6.5 and 5.5) in a dose-dependent manner when the cell was perfused with K-ECS. Figure 1b shows current traces recorded from CTLL-2 cells expressing Kv1.3 channels in K-ECS, pH 7.35 or K-ECS, pH 5.5. The inactivation of the Kv1.3 current is significantly faster at pH 5.5 than at pH 7.35. We determined the two time constants and their amplitudes in low pH_e and expressed them as the percentage of the control value (the respective values measured in pH 7.35). In K-ECS, pH 6.5 the peak current did not change, its magnitude was 102.6 ± 1.8% of the control ($n = 7$, $P = 0.2$). At pH 5.5 the peak current decreased to 94.7 ± 2.3% of the control ($n = 10$, $P = 0.044$), but the decrease was less drastic than the one induced by an identical pH change in S-ECS. At pH 6.5 the inactivation time constants did not change significantly (τ_s: 111.8 ± 8.4%, τ_f: 123.4 ± 15.0% of the control value, $n = 7$, $P = 0.212$ and 0.174, respectively, Fig. 1c). At pH 5.5 τ_s did not change (102.2 ± 11.1% of the control, $n = 10$, $P = 0.84$), while the value of τ_f was 127.7 ± 10.9% of the control ($n = 10$, $P = 0.024$, Fig. 1c). These relatively small changes of inactivation time constants cannot explain the faster inactivation at low pH_e, so we also compared the amplitudes of the two components.

The amplitude of the slow inactivating component (A_s) decreased in a dose-dependent manner with pH_e, A_s was 91.7 ± 2.2% ($n = 7$, $P = 0.008$) and 77.4 ± 4.6% ($n = 10$, $P < 0.001$) of the value at pH 7.35, when the cell was treated with S-ECS, pH 6.5 and 5.5, respectively. The amplitude of the fast inactivating component (A_f) increased significantly in both low-pH conditions, the value of A_f was 169.9 ± 23.7% ($n = 7$, $P = 0.026$) and 173.7 ± 17.9% ($n = 10$, $P = 0.003$) of the control at pH_e 6.5 and 5.5, respectively.

The relative weight of the slow component significantly decreased at low pH_e, the value of $A_s/(A_s + A_f)$ was 0.738 ± 0.018 at pH 6.5 ($n = 7$) and 0.651 ± 0.030 at pH 5.5 ($n = 9$) (Fig. 1d). Thus, the decreased relative weight of the slow inactivating component accounts for the faster inactivation at low extracellular pH_e.

The interpretation of the change of the biphasic inactivation kinetics using the parameters of a double exponential fit [A_s, τ_s, A_f, τ_f, $A_s/(A_s + A_f)$] is complicated, so we used an alternative method to express the change of the rate of inactivation. We calculated the area under curve for the leak-corrected traces and we subtracted the area corresponding to the non-inactivating current component (Fig. 2d). The ratio of this corrected area and the amplitude of the inactivating current component gives a "time constant-like" quantity, which is equal to the value of the inactivation time constant in the case of monophasic current decay and is inversely proportional to the overall rate of inactivation in case of currents with biphasic inactivation kinetics. We termed this quantity area/peak ratio (APPR). The advantage of this method is that it describes the inactivation process using only one parameter, so the interpretation of data is much clearer than using the parameters of a double exponential fit.

Using the APPR as a measure of the rate of inactivation kinetics we confirmed the acceleration of inactivation by low pH_e in high-external-K^+ conditions. The APPR was 308.9 ± 9.7 ms in K-ECS, pH 7.35 ($n = 12$), while lowering pH_e decreased the APPR to 92.1 ± 1.5% ($n = 7$, $P = 0.001$) and 82.5 ± 3.9% ($n = 9$, $P = 0.005$) of this value at pH 6.5 and 5.5, respectively.

$[K^+]_e$ dependence of the effect of pH_e changes

Because of the opposite effects of acidification of the extracellular solution at 5 mM and 150 mM $[K^+]_e$ we also carried out the measurement at intermediate K^+ concentrations of 20 and 40 mM. At these concentrations, reliable fits of the decay of the current traces could be obtained neither with single nor double exponential equations, so the APPR was used to describe the inactivation kinetics. The mean APPRs were 201.1 ± 23.6 ms ($n = 8$) at 20 mM $[K^+]_e$ and 229.4 ± 22.0 ms ($n = 6$) at 40 mM $[K^+]_e$. Upon switching from pH 7.35 to 5.5 in 20 mM K-ECS the inactivation was slowed, the APPR increased to 120.0 ± 4.7% of that measured at pH 7.35 ($n = 9$, $P = 0.003$, Fig. 2a, c). In case of 40 mM K-ECS the switch from pH 7.35 to 5.5 did not change the inactivation kinetics, the APPR was the 97.2 ± 4.4% of the control ($n = 8$, $P = 0.549$, Fig. 2b, c). For the sake of direct comparison of the inactivation kinetics at 20, 40 and 150 mM $[K^+]_e$ with those in S-ECS (5 mM $[K^+]_e$) we determined the APPRs for traces recorded in S-ECS solutions as well. In S-ECS, pH 7.35 the APPR was 131.6 ± 13.1 ms ($n = 16$). Lowering pH_e increased the APPR to 116.1 ± 3.8% ($n = 7$) and 133.2 ± 2.5% ($n = 5$) of the control at pH 6.5 and 5.5, respectively (Fig. 2c). These results do not differ from that obtained from the fit of the decay of current traces using single exponential function (Somodi et al. 2004).

Inward potassium current: reduced filling of the binding site from the intracellular side

The second possibility to increase the weight of external filling of the control site is to create conditions in which potassium ions flow inward through the channels. This could be accomplished by lowering the intracellular $[K^+]$. We first tried to lower the internal $[K^+]$ while keeping the

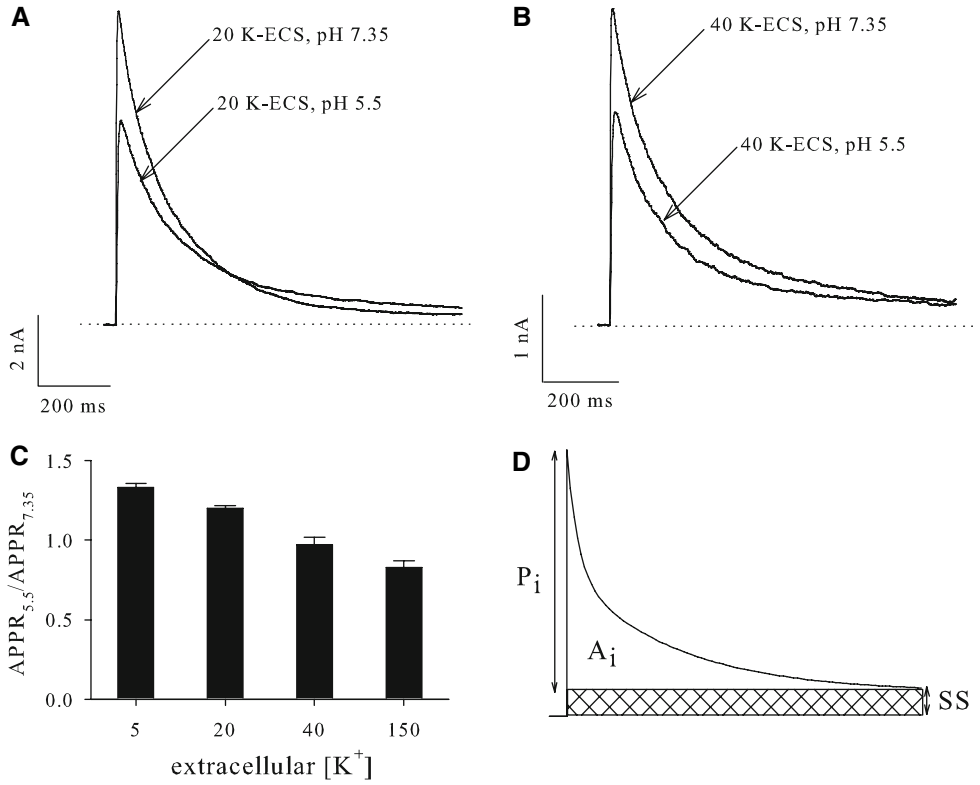

Fig. 2 $[K^+]_e$ dependence of acidification induced change in inactivation rate (**a**, **b**) K^+ currents of a CTLL-2 cell were recorded in whole-cell configuration during 2 s-long test pulses to +50 mV. The holding potential was −120 mV. Test pulses were applied every 60 s. The bath was perfused with control solutions (20 mM K-ECS, pH 7.35 for *panel a* and 40 mM K-ECS, pH 7.35 for *panel b*), and then with 20 mM K-ECS pH 5.5 (**a**) or with 40 mM K-ECS pH 5.5 (**b**). **c** Peak whole-cell currents and the area under the traces at +50 mV test potential were measured and the area/peak ratios were calculated at pH 7.35 ($APPR_{7.35}$) and at 5.5 ($APPR_{5.5}$, see text for details). The ratio of $APPR_{5.5}/APPR_{7.35}$ was calculated for different $[K^+]_e$-s. Error bars indicate SE. **d** Calculation of APPR. The inactivating component of the current amplitude (P_i) is calculated by subtracting the steady-state (SS) current level from the absolute peak. Similarly, the charge corresponding to the inactivating component (A_i, empty area) is obtained by integrating the current trace and subtracting the area (charge) contributed by the SS component (*cross hatched*). Then the A_i/P_i ratio is calculated

original S-ECS, but with these conditions, Kv1.3 channels collapsed and were not able to conduct potassium current. The probable reason is that the occupancy of potassium binding sites in the conductive pathway of the channel is critically low, which causes the collapse of the channel (Gomez-Lagunas 1997). The lowest $[K^+]_i$, which resulted in functional channels was 5 mM. With 5 mM $[K^+]_i$ we had to increase the extracellular $[K^+]$ to get inward current. In our experiments we used at least 20 mM extracellular $[K^+]$.

Our expectation was that due to the greater contribution of extracellular filling of the binding site the protonation of the histidines (H399) in low pH_e would lower the occupancy of the control site compared to the normal intracellular $[K^+]$ condition. The lower occupancy of the binding site results in faster inactivation kinetics according to our hypothesis.

Using 5 mM $[K^+]$ in the pipette the reversal potential for K^+ differs from the conventional −85 mV. When the cell was perfused with 20, 40 or 150 mM K-ECS the calculated reversal potential for potassium was +35.4, +53.1 and +87.3 mV, respectively. Since these values are close to +50 mV the driving force is very low at this voltage. Consequently, we used +20 mV test potentials to get greater driving force for the inward current and therefore higher current amplitude. Inward currents recorded in 20, 40 or 150 mM K-ECS are shown in Fig 3a–c, respectively. The complex inactivation kinetics of the currents was characterized by the APPR values in order to provide direct comparison of these results with those measured with 140 mM internal $[K^+]$. In 20 mM K-ECS the switch from pH 7.35 to 5.5 did not change the APPR (Fig. 3a, d, 101.7 ± 1.9% of the value at pH 7.35, $n = 13$, $P = 0.400$), while in 40 mM K-ECS the same switch decreased the ratio to 93.0 ± 2.1% of the control (Fig 3b, d, $n = 15$, $P = 0.005$).

When the cell was perfused with 150 mM K-ECS, pH 7.35 inactivation was clearly biphasic, the inactivation time constants were $\tau_s = 1186 \pm 217$ and $\tau_f = 131 \pm 30$ ms ($n = 3$), the proportion of the slow inactivating component was 0.511 ± 0.023 ($n = 3$). Application of 150 mM K-ECS, pH 5.5 accelerated inactivation kinetics (Fig 3c), but the

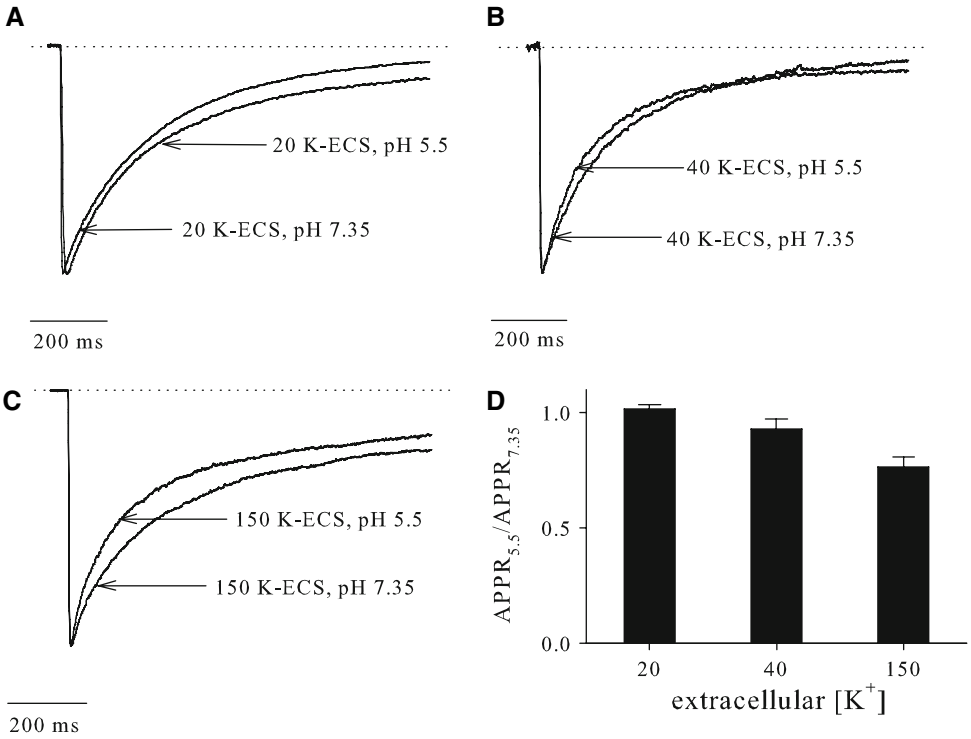

Fig. 3 $[K^+]_e$ dependence of acidification induced change in inactivation rate for inward currents (**a**–**c**) K^+ currents of CTLL-2 cells were recorded in whole-cell configuration during 2 s-long test pulses to +20 mV from a holding potential of −120 mV. Test pulses were applied every 60 s. The pipette solution contained 5 mM K^+, so reversal potentials for K^+ were more positive than +20 mV. The bath was perfused with 20 mM K-ECS, pH 7.35 (*panel a*), 40 mM K-ECS, pH 7.35 (*panel b*) or 150 mM K-ECS, pH 7.35 (*panel c*), and with solutions containing K^+ in the same concentration with pH 5.5. Currents were normalized for easier comparison of inactivation kinetics. **d** Peak whole-cell currents and the area under curve at +20 mV test potential were measured and the area/peak ratios were calculated at pH 7.35 ($APPR_{7.35}$) and at pH 5.5 ($APPR_{5.5}$). The ratio of $APPR_{5.5}/APPR_{7.35}$ was calculated for different $[K^+]_e$-s. *Error bars* indicate SE

inactivation time constants did not change (τ_s: 122.0 ± 29.0%, $P = 0.527$; τ_f: 84.6 ± 10.3%, $P = 0.273$; $n = 3$). The weight of the slow component $A_s/(A_s + A_f)$ decreased to 0.378 ± 0.020 at pH 5.5, which is responsible for the overall acceleration of inactivation. For direct comparison of these data with the ones obtained at intermediate $[K^+]_e$, the APPR vales were also calculated. The APPR was 271.3 ± 16.8 ms at pH 7.35 and the switch to pH 5.5 reduced it significantly 76.6 ± 3.2% of the control (Fig. 3d, $n = 3$, $P = 0.018$). Overall, the effect of the pH switch on the rate of inactivation of inward currents was dependent on $[K^+]_e$, showing pronounced acceleration with increasing $[K^+]_e$ (Fig. 3d).

The results mentioned above indicate that when the contribution of filling of the critical binding site from the extracellular side of the pore is increased, the rate of inactivation in response to extracellular acidification is increased in contrast to the slowing observed in physiological conditions.

Low extracellular pH slows the wash-in kinetics of barium ions

In order to further examine ion entry into the pore from the extracellular side we used barium ions. Barium ions are able to enter the pore of various K^+ channels, but they are bound more strongly inside the permeation pathway because of their divalent nature. The slow permeation of barium ions hinders the permeation of potassium ions, which causes an apparent block of K^+ current. We showed in our earlier results that in Kv1.3 channels the electrical barrier generated by the positively charged side chains of the amino acid residues at position 399 (protonated histidines or lysines) impedes the exit of Ba^{2+} ions from the channel on the basis of wash-out kinetics of Ba^{2+} ions after block at different pH values. This time our aim was to investigate how the entry rate of Ba^{2+} ions into the pore is affected by changes in pH_e.

Since the frequency of test pulses that can be applied to Kv1.3 channels is limited by cumulative inactivation it is difficult to resolve small changes in the fast wash-in kinetics of barium. This prompted us to modify our original protocol to improve the temporal resolution. As Ba^{2+} block of K^+ channels is voltage dependent we used a less negative (−90 mV) holding potential and more positive (+70 mV) depolarizing pulses to delay the entry of barium ions into the pore (Harris et al. 1998). In addition, we decreased the duration of the depolarizing pulses (the duration of channel

opening) to 10 ms. The use of such short depolarizing pulses enabled us to apply them every 15 s without cumulative inactivation.

Application of 15 mM Ba^{2+} in S-ECS reduced K^+ currents of Kv1.3 channels to 39.1 ± 2.9% ($n = 6$) and 17.9 ± 1.4% ($n = 6$) of the control at pH 7.35 and 5.5, respectively. Figure 4a and b show that the wash-in kinetics was significantly slower at pH 5.5 than at pH 7.35, the time constant of wash-in was 32.8 ± 1.4 ($n = 7$) and 46.5 ± 2.6 s ($n = 6$) at pH 7.35 and 5.5, respectively ($P < 0.001$, Fig. 4c). Pairwise cell-by-cell comparison yielded a similar result: the time constant increased in low pH_e to 137.3 ± 2.8% of the control value ($n = 6$, $P < 0.001$).

The kinetics of Ba^{2+} block was also measured in mutant channels with a neutral residue (L) or a permanently positively charged residue (K) in the critical 399 position at pH 7.35 and 5.5. 15 mM Ba^{2+} caused a significantly higher block of the mutant channels than the wild-type channels, and the wash-in kinetics was too fast to resolve. Since the Ba^{2+} association rate is proportional to its concentration we reduced the association rate by applying Ba^{2+} at only 5 mM. The remaining current fractions in the presence of 5 mM Ba^{2+} were 34.3 ± 1.28 ($n = 6$) and 32.1 ± 1.04% ($n = 6$) for the H399L mutant, and 17.4 ± 0.71 ($n = 6$) and 13.0 ± 1.2% ($n = 5$) for the H399K mutant at pH 7.35 and 5.5, respectively. For the H399L mutant the wash-in time constants were 18.1 ± 0.6 s ($n = 5$) and 18.3 ± 0.6 s ($n = 6$) at pH 7.35 and 5.5, respectively (Fig 4d). The corresponding values for the H399K mutant were 25.51 ± 1.12 s ($n = 6$) at pH 7.35 and 26.95 ± 0.92 s ($n = 5$) at pH 5.5 (Fig 4d). Statistical analysis (ANOVA supplemented with Bonferroni t test) of the results showed that the time constants at pH 7.35 and 5.5 differed neither for the H399L nor for the H399K mutant, but wash-in kinetics were signifi-

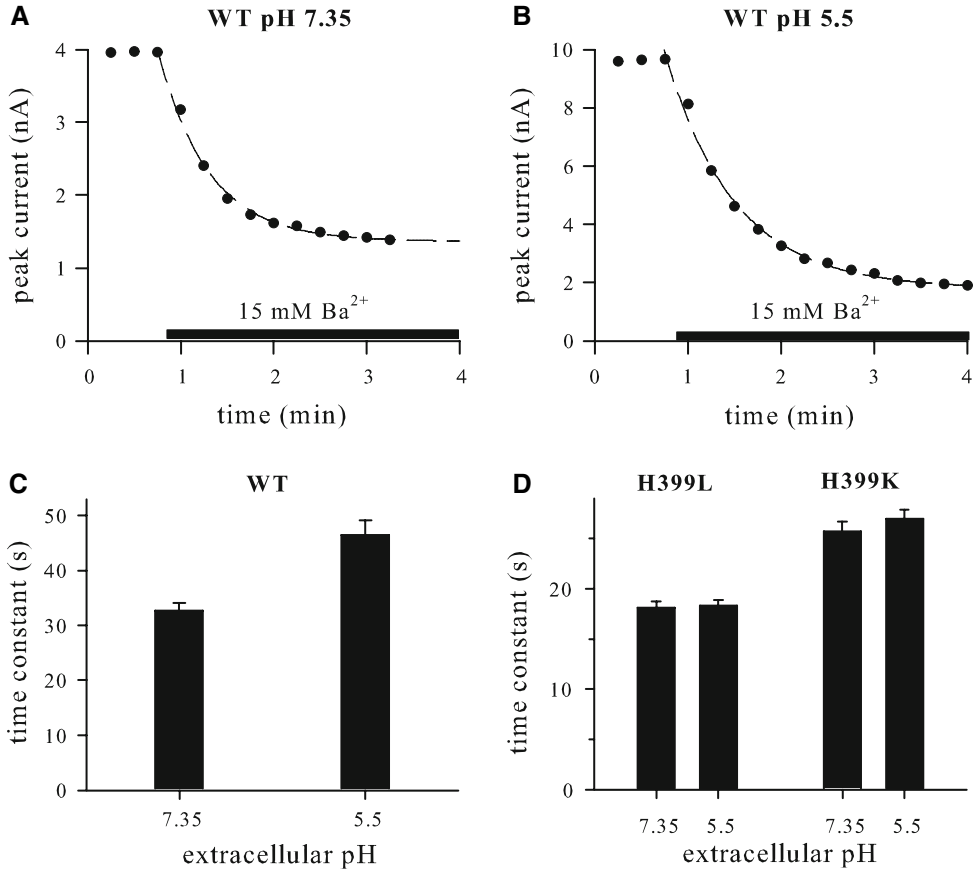

Fig. 4 Wash-in kinetics of Ba^{2+} block in wild type, H399L and H399K mutant channels. **a**, **b** Reduction of extracellular pH slows the wash-in kinetics of Ba^{2+} block in wild type Kv1.3 channels. Currents were recorded in whole-cell configuration during 10-ms-long test pulses to +70 mV. The holding potential was −90 mV. Test pulses were applied every 15 s. The panels show the peak currents under different ionic conditions. The bath was perfused with control solution S-ECS pH 7.35 (**a**) and S-ECS pH 5.5 (**b**) and with the same solution containing 15 mM Ba^{2+} (*black stripe* above the time axis indicates the duration of Ba^{2+} application). The *superimposed dashed lines* show single-exponential fits to the wash-in kinetics. The wash-in time constants for the cells shown were 32.0 and 45.0 s at pH 7.35 and 5.5, respectively. Wash-in time constants for the wild type (**c**) and for the H399L and H399K mutant (**d**) channels at pH 7.35 and at 5.5. In the case of mutant channels the experimental conditions were the same as in wild-type channels, but the holding potential was −120 mV and the Ba^{2+} concentration was 5 mM. *Error bars* indicate SE

cantly faster for H399L than for H399K channels at both pH values.

Discussion

The Kv1.3 potassium channel has been known to slow its inactivation rate upon exposure to low pH_e in contrast to the acceleration seen in other related channels (Deutsch and Lee 1989; Perez-Cornejo 1999; Kehl et al. 2002; Starkus et al. 2003; Li et al. 2003; Somodi et al. 2004). In our previous study we identified the H399 residue to be responsible for this anomalous behavior and constructed a model to explain the mechanism. The main concept of the model is that in low extracellular pH the protonated histidine residues in position 399 create an electric potential barrier, which hinders the exit of K^+ ions from the pore of the channel to the extracellular space. The hindered exit rate results in the higher occupancy of the control site and the slowing of inactivation.

The effect of the extracellular ionic composition, especially K^+ concentration, on the rate of slow inactivation of K^+ channels has been also known for long. The slowing of the inactivation rate in high $[K^+]_e$ is attributed to the increased occupancy of a control site by K^+ ions in the selectivity filter. The inactivation of Kv1.3 channels is also slowed by high $[K]_e$ and becomes biphasic. Under these conditions, lowering pH_e to 5.5 accelerated inactivation as opposed to the slowing observed in low $[K]_e$. In the current study, we reconcile this result with our existing model and gather more supportive evidence for its validity.

Simply assuming that the electric field of the protonated histidines at the extracellular entrance of the pore represents a potential barrier for cations both on their way into or out of the pore, the expected consequence is that the increased filling of the control site from the extracellular side provided by the high K^+ concentration is hampered. As a result the occupancy of the site is decreased and inactivation rate is increased. Thus, no additional assumptions are needed to make the model more complex; it is compatible with the observation that the rate of inactivation is accelerated, provided that the significance of external filling of the control site is increased.

As acidification induced opposite effects on the inactivation rate at 5 and 140 mM $[K^+]_e$ we examined the effect of low pH_e at intermediate K^+ concentrations. The direct comparison of the inactivation rates in various conditions, which often deviated from a simple single exponential decay, was made possible by the introduction of the quantity termed APPR, which gives the ratio of the total charge under the inactivating component of the current trace and the amplitude of the inactivating component. The result is a quantity measured in time units that serves as an "overall time constant" to describe the rate of current decay due to inactivation. Using APPR, we found that at $[K^+]_e < 40$ mM the inactivation rate was slowed by low pH_e, it was enhanced at $[K^+]_e = 150$ mM and was not changed at 40 mM. This is clearly demonstrated in Fig. 2c by the ratios of the APPRs determined at pH 5.5 and 7.35 at various $[K^+]_e$: the ratio is greater than 1 at $[K^+]_e = 5$ and 20 mM, is about 1 at $[K^+]_e = 40$ mM and less than 1 at $[K^+]_e = 150$ mM. The figure shows the tendency from slowing to acceleration as the significance of external filling of the control site increases.

Our model suggests that in conditions when the control site is mostly filled by K^+ from the extracellular side, protonation of the histidine side chains will cause acceleration of the inactivation. Besides raising $[K^+]_e$, we aimed to test this hypothesis by keeping $[K^+]_e$ at the physiological 5 mM and inducing inward currents. We assumed that even if $[K^+]_e$ is kept low, K^+ ions representing inward current should encounter the electrostatic barrier of the histidines as they are entering the pore from the outside and this should be apparent in the accelerated rate of inactivation. However, K^+ channels are known to lose their conductance in very low potassium concentrations due to the restructuring of the selectivity filter (Zhou et al. 2001; Gomez-Lagunas 1997), and accordingly, lowering the internal $[K^+]$ to below 5 mM resulted in no measurable current. Consequently, we modified our solutions and protocol to suit the goal of the experiment: 5 mM internal and 20 mM external $[K^+]$ were used along with depolarizing pulses to +20 mV to obtain inward currents.

At $[K^+]_e = 20$ mM with normal intracellular solution the inactivation rate of the outward current was significantly slowed by the switch from pH 7.35 to 5.5. However, at the same $[K^+]_e$ the inactivation rate was unchanged by the pH switch when currents were inward. With 5 mM K^+ in the pipette raising $[K^+]_e$ produced a tendency similar to that observed for high $[K^+]_i$: with the increasing weight of extracellular filling acceleration of the inactivation rate upon lowering pH_e became more pronounced. Thus, increasing $[K^+]_e$ resulted in an overall shift from slowing (or no change) to acceleration in inactivation rate with the switch to low pH_e, regardless of the intracellular $[K^+]$ used (compare Figs. 2c, 3d). However, the "turning point", the extracellular K^+ concentration at which the pH_e switch induces no change in the inactivation rate because it represents the transition from slowing to acceleration, was shifted toward lower $[K^+]_e$ when inward currents were measured, as expected from the model. Obviously, at lower $[K^+]_i$ and inward currents a lower $[K^+]_e$ is sufficient to supply the K^+ ions for filling the control site from the extracellular side.

In our previous study we demonstrated the delayed exit of barium ions from wild-type Kv1.3 channels in low pH_e,

as well as the pH_e-insensitive exit of Ba^{2+} from the mutants H399K and H399L, whose side chains at position 399 are not protonated upon the switch from pH_e 7.35 to 5.5 (Somodi et al. 2004). Considering the filling of the control site from the outside, our model predicts that positively charged side chains at the extracellular entrance of the pore should hinder the entry of Ba^{2+} as well, which could be detected as slower wash-in kinetics, when the histidines are protonated. Our results confirmed this expectation: block of the channels by barium was significantly slower in low pH_e. Furthermore, wash-in kinetics were pH_e-insensitive for both mutants with non-titratable residues at position 399, supporting the assumption that it is the charge gained by protonation of H399 that modifies Ba^{2+} entry rate. It is also noteworthy that wash-in kinetics of H399K bearing a positive side chain had slower kinetics than H399L with a neutral side chain. Their direct comparison, however, may not be relevant since besides the charge, the length and structure of their side chains are also different, and even conservative mutations at this position are known to induce great changes in inactivation rate (López-Barneo et al. 1993; Somodi et al. 2004).

Although the focus of this study was the effect of pH_e on the inactivation rate, it cannot go unnoticed that the current amplitude was also reduced upon acidification in physiological solutions. This phenomenon has been reported for Shaker and several related mammalian channels (Kehl et al. 2002; Starkus et al. 2003; Somodi et al. 2004). Internal protons were shown to directly block Shaker channels, but low pH_e was found to reduce current amplitude via accelerated inactivation only (Starkus et al. 2003). The opposite conclusion was reached for Kv1.5 channels: even though the involvement of an inactivation mechanism was proposed based on the sensitivity of current inhibition to $[K^+]_e$ and the identity of the Shaker 449 equivalent residue, it could not account for the decrease in current amplitude alone (Kehl et al. 2002). Our present results reinforce this observation in Kv1.3, since in high $[K^+]_e$ hardly any current amplitude decrease was detected, while the inactivation rate was significantly increased. These facts suggest a link, but not a direct consequential one, between enhanced slow inactivation and amplitude decrease. A recent study using voltage-clamp fluorimetry proposes a resolution of this question by concluding that in addition to the acceleration of P/C-type inactivation the major mechanism of pH_e-induced current inhibition is the inactivation of channels from closed states from which they can activate, but not open (Claydon et al. 2007).

A mechanism similar to the main hypothesis of our model was suggested to explain the role of a lysine residue in the turret region of rat Kv2.1 channels (K356, equivalent of Shaker 425) in K^+ permeation (Consiglio et al. 2003). The side chain of this lysine was found to interfere with the K^+ dehydration/rehydration site located outside of the selectivity filter (Zhou et al. 2001) in the outer vestibule and make the K^+ exit from the selectivity filter in the outward direction rate limiting. In addition, similar to our model, this interference with the passage of K^+ ions was also symmetrical, that is, the entry of K^+ ions into the selectivity filter from the outside was hindered as well. This effect seemed independent of the Y380 residue (H399 in hKv1.3 and T449 in Shaker) and the authors found the interaction between these two residues in the phenomenon unlikely.

In agreement with our model another study also proposed that the charge of residue R487 of hKv1.5 channels (H399 in hKv1.3 and T449 in Shaker) influenced the occupancy of the outermost K^+ binding site in the selectivity filter, thereby controlling permeation (Jager and Grissmer 2001). These results, however, suggested an interaction between H463 (equivalent of Shaker 425) and R487, the protonation of the former changing the effective charge of the latter, which in turn affected the binding site. The interaction between these residues and their combined effect on inactivation was also reported by others (Zhang et al. 2005). More recently it was shown that mutations of H463 to residues of different charge and size had similar effects on channel function, so a pure electrostatic interaction with R487 was ruled out (Eduljee et al. 2007).

Thus, channels bearing a positively charged residue at the Shaker 425 equivalent position may directly influence permeation very much like we propose here the protonated H399 influences the rate of inactivation, the main difference being the location of the affected K^+ binding sites. Furthermore, that residue in the outer vestibule may interact with the selectivity filter via the residue homologous to hKv1.3 H399 and indirectly affect permeation and slow inactivation. All these findings indicate that these two residues are major determinants of the electrostatic landscape of the outer pore region and as such have a major role in controlling K^+ permeation and inactivation. The hKv1.3 channel examined here has a glycine at position 375 (the equivalent of Shaker 425), which is unlikely to be involved in any of such interactions due to the small size an neutral nature of its side chain, so the residue at position 399 may be even more dominant in this channel.

In conclusion, we have previously established a model to describe the role of residue H399 in the pH_e-dependence of the slow inactivation of hKv1.3 in physiological conditions. Here we tested and confirmed the validity of the model in elevated $[K^+]_e$ conditions and for inward K^+ currents. The results presented in these two studies support our hypothesis that an electrostatic potential barrier is created at the external mouth of the pore by the protonation of the H399 residues in low pH_e, which is encountered by K^+ ions both entering and exiting the pore. In the case of physiological

K^+ concentrations and outward currents this barrier increases the occupancy of the binding site and slows inactivation, while in cases when the site is mostly filled by K^+ ions from the outside, such as high-$[K^+]_e$ conditions and inward currents, the barrier decreases occupancy and thus enhances inactivation.

The model we propose qualitatively describes the phenomenon of modulation of the inactivation kinetics of Kv1.3 by pH_e and $[K]_e$. In the absence of a coherent model for the bi-exponential inactivation kinetics in high $[K]_e$ (i.e. number of states and transitions between them and the number of K^+ binding sites involved are not known) it is also possible to imagine that the increasing $[K]_e$ influences the gating behavior of Kv1.3 through multiple mechanisms. For example, there might be two regulatory K^+ binding sites accessible from the extracellular space, one controlling the collapse of the outer pore, whereas the other controlling the distribution of K^+ channels between gating modes having distinctly different inactivation and conduction properties as a function of pH_e. The discrimination between these scenarios would require a mathematical model of Kv1.3 inactivation at high $[K^+]_e$ and experimental conditions where rate constants could be determined to characterize inactivation, rather than the APPR as done in our study.

Although our simple model, in which H399 has a central role, can account for the anomalous change in inactivation upon lowering pH_e, H399 is probably not the sole determinant of inactivation rate in hKv1.3. The acceleration of inactivation in low pH_e seen in numerous related channels is most likely present in hKv1.3 too, since several of its H399 mutants behave the same way (Somodi et al. 2004). The protonation of Shaker D447 in the selectivity filter or its equivalent residues in other channels have been suggested to be responsible for this effect (Starkus et al. 2003; Eduljee et al. 2007), which may be overridden by the electrostatic effect of H399 in hKv1.3.

Acknowledgments We thank the careful technical assistance of Cecila Nagy. This study was supported by Hungarian grants OTKA K60740, K73080, NK61412 and ETT 068/2006.

References

Andalib P, Consiglio JF, Trapani JG, Korn SJ (2004) The external TEA binding site and C-type inactivation in voltage-gated potassium channels. Biophys J 87:3148–3161

Baukrowitz T,Yellen G (1995) Modulation of K^+ current by frequency and external [K+]: a tale of two inactivation mechanisms. Neuron 15:951–960

Baukrowitz T,Yellen G (1996) Use-dependent blockers and exit rate of the last ion from the multi-ion pore of a K^+ Channel. Science 271:653–656

Busch AE, Hurst RS, North RA, Adelman JP, Kavanaugh MP (1991) Current inactivation involves a histidine residue in the pore of the rat lymphocyte potassium channel RGK5. Biochem Biophys Res Commun 179:1384–1390

Choi KL, Aldrich RW, Yellen G (1991) Tetraethylammonium blockade distinguishes two inactivation mechanisms in voltage-activated K^+ channels. Proc Natl Acad Sci USA 88:5092–5095

Claydon TW, Boyett MR, Sivaprasadarao A, Ishii K, Owen JM, O'Beirne HA, Leach R, Komukai K, Orchard CH (2000) Inhibition of the K+ channel kv1.4 by acidosis:protonation of an extracellular histidine slows the recovery from N-type inactivation. J Physiol 526(Pt 2):253–264

Claydon TW, Boyett MR, Sivaprasadarao A, Orchard CH (2002) Two pore residues mediate acidosis-induced enhancement of C-type inactivation of the Kv1.4 K(+) channel. Am J Physiol Cell Physiol 283:C1114–C1121

Claydon TW, Makary SY, Dibb KM, Boyett MR (2004) K+ activation of kir3.1/kir3.4 and kv1.4 K+ channels is regulated by extracellular charges. Biophys J 87:2407–2418

Claydon TW, Vaid M, Rezazadeh S, Kwan DC, Kehl SJ, Fedida D (2007) A direct demonstration of closed-state inactivation of K+ channels at low pH. J Gen Physiol 129:437–455

Consiglio JF, Andalib P, Korn SJ (2003) Influence of pore residues on permeation properties in the Kv2.1 potassium channel. Evidence for a selective functional interaction of K+ with the outer vestibule. J Gen Physiol 121:111–124

Deutsch C, Chen L-Q (1993) Heterologous expression of specific K^+ channels in T lymphocytes: functional consequences for volume regulation. Proc Natl Acad Sci USA 90:10036–10040

Deutsch C, Lee SC (1989) Modulation of K^+ currents in human lymphocytes by pH. J Physiol (Lond) 413:399–413

Eduljee C, Claydon TW, Viswanathan V, Fedida D, Kehl SJ (2007) SCAM analysis reveals a discrete region of the pore turret that modulates slow inactivation in Kv1.5. Am J Physiol Cell Physiol 292:C1041–C1052

Fedida D, Maruoka ND, Lin S (1999) Modulation of slow inactivation in human cardiac Kv1.5 channels by extra- and intracellular permeant cations. J Physiol 515(Pt 2):315–329

Gomez-Lagunas F (1997) Shaker B K+ conductance in Na+ solutions lacking K+ ions: a remarkably stable non-conducting state produced by membrane depolarizations. J Physiol 499(Pt 1):3–15

Grissmer S,Cahalan MD (1989) Divalent ion trapping inside potassium channels of human T lymphocytes. J Gen Physiol 93:609–630

Hamill OP, Marty A, Neher E, Sakmann B, Sigworth FJ (1981) Improved patch-clamp techniques for high-resolution current recording from cells and cell-free membrane patches. Pflugers Arch 391:85–100

Harris RE, Larsson HP, Isacoff EY (1998) A permanent ion binding site located between two gates of the Shaker K+ channel. Biophys J 74:1808–1820

Heginbotham L,MacKinnon R (1992) The aromatic binding site for tetraethylammonium ion on potassium channels. Neuron 8:483–491

Hoshi T, Zagotta WN, Aldrich RW (1990) Biophysical and molecular mechanisms of Shaker potassium channel inactivation [see comments]. Science 250:533–538

Hoshi T, Zagotta WN, Aldrich RW (1991) Two types of inactivation in Shaker K^+ channels:effects of alterations in the carboxy-terminal region. Neuron 7:547–556

Jager H, Grissmer S (2001) Regulation of a mammalian Shaker-related potassium channel, hKv1.5, by extracellular potassium and pH. FEBS Lett 488:45–50

Kehl SJ, Eduljee C, Kwan DC, Zhang S, Fedida D (2002) Molecular determinants of the inhibition of human Kv1.5 potassium currents by external protons and Zn(2+). J Physiol 541:9–24

Kiss L,Korn SJ (1998) Modulation of C-type inactivation by K+ at the potassium channel selectivity filter. Biophys J 74:1840–1849

Kiss L, LoTurco J, Korn SJ (1999) Contribution of the selectivity filter to inactivation in potassium channels. Biophys J 76:253–263

Li X, Bett GC, Jiang X, Bondarenko VE, Morales MJ, Rasmusson RL (2003) Regulation of N- and C-type inactivation of Kv1.4 by pHo and K+: evidence for transmembrane communication. Am J Physiol Heart Circ Physiol 284:H71–H80

Liu Y, Jurman ME, Yellen G (1996) Dynamic rearrangement of the outer mouth of a K^+ channel during gating. Neuron 16:859–867

Loots E, Isacoff EY (1998) Protein rearrangements underlying slow inactivation of the Shaker K+ channel. J Gen Physiol 112:377–389

Loots E, Isacoff EY (2000) Molecular coupling of S4 to a K+ channel's slow inactivation gate. J Gen Physiol 116:623–635

López-Barneo J, Hoshi T, Heinemann SH, Aldrich RW (1993) Effects of external cations and mutations in the pore region on C-type inactivation of *Shaker* potassium channels. Recept Channels 1:61–71

Matteson DR, Deutsch C (1984) K channels in T lymphocytes: a patch clamp study using monoclonal antibody adhesion. Nature 307:468–471

Neyton J, Miller C (1988) Discrete Ba2+ block as a probe of ion occupancy and pore structure in the high-conductance Ca2+ -activated K+ channel. J Gen Physiol 92:569–586

Nguyen AN, Kath JC, Hanson DC, Biggers MS, Cannif PC, Donovan CB, Mather RJ, Bruns MJ, Rauer H, Aiyar J, Lepple-Wienhues A, Gutman GA, Grissmer S, Cahalan MD, Chandy KG (1996) Novel nonpeptide agents potently block the C-type inactivated conformation of Kv1.3 and suppress T cell activation. Mol Pharmacol 50:1672–1679

Ogielska EM, Aldrich RW (1999) Functional consequences of a decreased potassium affinity in a potassium channel pore. Ion interactions and C-type inactivation. J Gen Physiol 113:347–358

Olcese R, Latorre R, Toro L, Bezanilla F, Stefani E (1997) Correlation between charge movement and ionic current during slow inactivation in Shaker K+ channels. J Gen Physiol 110:579–589

Perez-Cornejo P (1999) H+ ion modulation of C-type inactivation of Shaker K+ channels. Pflugers Arch 437:865–870

Rasmusson RL, Morales MJ, Castellino RC, Zhang Y, Campbell DL, Strauss HC (1995) C-type inactivation controls recovery in a fast inactivating cardiac K+ channel (Kv1.4) expressed in Xenopus oocytes. J Physiol 489(Pt 3):709–721

Somodi S, Varga Z, Hajdu P, Starkus JG, Levy DI, Gaspar R, Panyi G (2004) pH dependent modulation of Kv1.3 inactivation: the role of His399. Am J Physiol Cell Physiol 287:C1067–C1076

Starkus JG, Varga Z, Schonherr R, Heinemann SH (2003) Mechanisms of the inhibition of Shaker potassium channels by protons. Pflugers Arch 447:44–54

Steidl JV, Yool AJ (1999) Differential sensitivity of voltage-gated potassium channels Kv1.5 and Kv1.2 to acidic pH and molecular identification of pH sensor. Mol Pharmacol 55:812–820

Yellen G (1998) The moving parts of voltage-gated ion channels. Q Rev Biophys 31:239–295

Zagotta WN, Hoshi T, Aldrich RW (1990) Restoration of inactivation in mutants of Shaker potassium channels by a peptide derived from ShB [see comments]. Science 250:568–571

Zhang S, Eduljee C, Kwan DC, Kehl SJ, Fedida D (2005) Constitutive inactivation of the hKv1.5 mutant channel, H463G, in K+-free solutions at physiological pH. Cell Biochem Biophys 43:221–230

Zhou Y, Morais-Cabral JH, Kaufman A, MacKinnon R (2001) Chemistry of ion coordination and hydration revealed by a K+ channel-Fab complex at 2.0 A resolution. Nature 414:43–48